

Quantum kinetic exciton-LO-phonon interaction in CdSe

U. Woggon, F. Gindele, and W. Langbein

FB Physik, Universität Dortmund, Otto-Hahn-Strasse 4, D-44227 Dortmund, Germany

J. M. Hvam

Research Center COM, Technical University of Denmark, DK-2800 Lyngby, Denmark

(Received 27 July 1999)

Oscillations with a period of ~ 150 fs are observed in the four-wave mixing (FWM) signal of bulk CdSe and interpreted in terms of non-Markovian exciton-LO-phonon scattering. The experiments show evidence of phonon quantum kinetics in semiconductors of strong polar coupling strength and high exciton binding energy. By comparison of the spectral and temporal response of the FWM signal in bulk CdSe and CdSe quantum dots, we demonstrate the influence of continuum states on the interference of electron-hole pair polarizations coupled via an LO phonon.

I. INTRODUCTION

In a semiclassical treatment of light-matter interaction, the time evolution of a system coupled to a bath is generally described by two damping constants T_1 for the energy relaxation and T_2 for the phase relaxation time. Such an approach is a common practice, e.g., in the density matrix formalism or when solving the optical Bloch equations (see, e.g., Refs. 1–3 and references therein). If the system can be described by a Lorentzian oscillator, the homogeneous line broadening Γ in the spectrum is given by $\Gamma = 2\hbar/T_2$ and the decay of polarization proceeds in a strictly exponential form. In that model, scattering processes are considered as infinitely short in time. Such an impact approximation, however, results in pronounced tails in the spectral line shape that are usually not observed. On a short time scale, scattering processes are not yet completed and the dynamics of the system is connected to the history at earlier times. The time evolution of the system depends on its state at times $t' \leq t$, i.e., memory effects have to be taken into account by replacing the damping constants Γ by $\Gamma(t-t')$ and integrating over all previous states of the system. For such a case the dynamics is called non-Markovian.^{3–6}

In semiconductors, the time evolution of the electronic states is given by a many-particle Schrödinger equation that cannot be solved analytically. The decay of polarization is mediated by carrier-carrier scattering and carrier-phonon scattering. If the exciting laser pulses are as short as the collision times, memory effects can no longer be neglected and the relaxation dynamics of the semiconductor has to be described by quantum kinetics. Evidence for non-Markovian electron-LO-phonon scattering has been obtained in two-beam four-wave mixing (FWM) experiments on bulk GaAs.⁷ The time-integrated FWM signal exhibits oscillations of ~ 100 fs, a time slightly below the LO-phonon oscillation period of $T_{LO} = 2\pi/\omega_{LO} = 115$ fs in GaAs. In the spectral response, however, no corresponding LO-phonon sidebands are found. Such a behavior has been predicted by theory as being a typical signature of LO-phonon quantum kinetics in semiconductors.⁸ The observed renormalization of the oscil-

lation period $\bar{T}_{osc} = 2\pi/\bar{\omega}_{osc}$ according to $\bar{\omega}_{osc} = \omega_{LO}(1 + m_e/m_h)$, where $m_{e,h}$ are the electron and hole masses, has been explained within a single-particle picture for small Fröhlich coupling constants $\alpha \ll 1$ and small exciton binding energies $E_{Ry} \ll \hbar\omega_{LO}$. Non-Markovian dynamics of LO-phonon scattering is also found in pump-and-probe experiments on bulk GaAs.⁹ Interest has now been focused on II-VI semiconductor compounds because of their larger Fröhlich coupling constants. The first experiments on ZnSe showed that the oscillations of the FWM signal are modulated by several beating frequencies, e.g., heavy-hole-light-hole (hh-lh) beating due to strain splitting or modulations by twice the LO-phonon oscillation period.¹⁰ In order to resolve the characteristic LO-phonon oscillations, coherent control experiments were implemented.¹¹ Currently, no quantum kinetic theory exists for the exciton-LO-phonon interaction in the strong coupling regime. The available theoretical models are developed for III-V semiconductors with small α and E_{Ry} . For strong polar coupling and large exciton binding energies, as typically found in II-VI materials, the consequences of non-Markovian relaxation on the spectral and temporal response of the FWM signal are still unknown.

In this paper, we study the time evolution of quantum coherence in the II-VI semiconductor CdSe by time-integrated, two-beam four-wave mixing, using spectrally tunable fs pulses of varying pulse length (70–200 fs). Since the carrier-LO-phonon and carrier-carrier interaction times are set by the LO-phonon period $T_{LO} = 2\pi/\omega_{LO} = 160$ fs ($\hbar\omega_{LO} = 25.9$ meV) and the plasma oscillation period $T_{pl} = 2\pi/\omega_{pl} \sim 200$ fs (for an electron-hole density of $n_{eh} = 1 \times 10^{17}$ cm⁻³), the carrier dynamics in CdSe enters the time regime of quantum kinetics already at pulse lengths of the exciting laser around 100 fs. The oscillation period of the FWM signal is analyzed, and the spectral response is studied. The oscillations found cannot be explained by a renormalized oscillation time as reported for GaAs, which points to the importance of excitonic effects. By extending the pulse length, the transition to the Markov limit is demonstrated. The results derived for bulk CdSe will be contrasted with those for CdSe quantum dots, a system of only discrete states

with even higher exciton binding energy and similar coupling strength to LO phonons. For both materials, the obtained results deviate from those measured for the electron-LO-phonon quantum kinetics in the weak coupling limit in GaAs. The differences are attributed to Coulomb correlation effects, in particular due to the higher exciton binding energies.

II. SAMPLES AND EXPERIMENTAL CONDITIONS

A. The material system CdSe

CdSe is a polar II-VI semiconductor of wurtzite crystal lattice structure with a band gap energy of 1.84 eV (at $T = 4$ K). The uppermost valence band is split by the crystal-field interaction, giving rise to two exciton series, labeled A and B, and separated in energy by $\Delta E_{AB} = 25$ meV. The spin-orbit split-off C valence band is well separated in energy by ~ 420 meV. The exciton binding energies are 15 meV and 16 meV for the A and B excitons, respectively. While the B exciton is optically allowed for both polarizations $\vec{E} \perp \vec{c}$ and $\vec{E} \parallel \vec{c}$, the A exciton is dipole-forbidden for the latter case (here \vec{c} is the crystal axis, \vec{E} the electric field). The A-biexciton binding energy of 4–5 meV has been determined by FWM experiments on a ps time scale.^{12,13} The Fröhlich-coupling constant α of CdSe is 0.39 and in the strong coupling regime (for comparison $\alpha_{\text{GaAs}} = 0.06$). The zone-center LO-phonon energy of 210 cm^{-1} is known from Raman scattering and corresponds to $\hbar\omega_{\text{LO}} = 25.9$ meV, or an oscillation period of $T_{\text{LO}} = 2\pi/\omega_{\text{LO}} = 160$ fs. The quantum kinetic model of the LO-phonon interaction, derived for GaAs,⁷ would predict for the corresponding CdSe material parameters a renormalized LO-phonon oscillation period of $\bar{T}_{\text{osc}} = 2\pi/\bar{\omega}_{\text{osc}} = 126$ fs of the FWM signal.

For the experiments, CdSe platelets of thickness $d \approx 1 \text{ } \mu\text{m}$ with an in-plane \vec{c} axis and CdSe quantum dots of $R = 2.5 \text{ nm}$ embedded in a glass matrix are used.

B. FWM and pulse shaping

The FWM signal is detected spectrally resolved and time-integrated in direction $2\vec{q}_2 - \vec{q}_1$ as function of delay time between the two exciting beams of directions \vec{q}_1 and \vec{q}_2 , using reflection geometry for bulk CdSe and transmission geometry for CdSe quantum dots. The fs pulses are provided by an optical parametric amplifier pumped by an amplified Ti:sapphire laser and can be spectrally tuned between 500 nm (2.48 eV) and 700 nm (1.77 eV). The excitation density can be adjusted between 10^{15} cm^{-3} and 10^{18} cm^{-3} . The laser pulses with a spectral width of ~ 25 meV [full width at half maximum (FWHM)] cover the energy range between the exciton energy E_X and $E_X + \hbar\omega_{\text{LO}}$. To extract the typical features of LO-phonon quantum kinetics, the superposition of coherent oscillations arising from different excitonic states has to be avoided. To suppress the excitation of interfering states which could produce disturbing quantum beats, we exploit the polarization selection rules and use external pulse shaping. By a grating/lens combination (pulse shaper), the spectral bandwidth of the exciting laser is controlled and the chirp is compensated to a minimum time-bandwidth

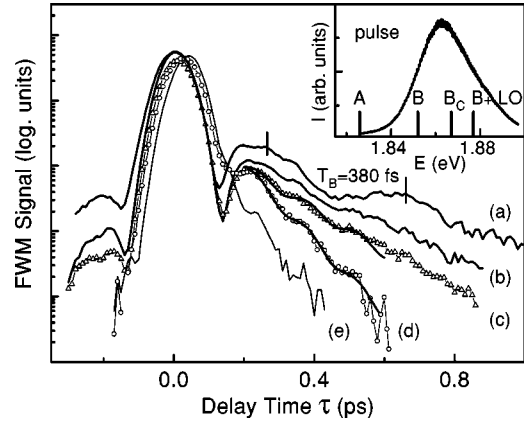


FIG. 1. Time-integrated FWM signal as a function of delay time excited by 70 fs pulses of polarization $\vec{E} \parallel \vec{c}$ and detected at the energy of the B exciton $E_B = 1.852$ eV. The excitation densities are (a) $4 \times 10^{15} \text{ cm}^{-3}$, (b) $3 \times 10^{16} \text{ cm}^{-3}$, (c) $1 \times 10^{17} \text{ cm}^{-3}$, (d) $3.7 \times 10^{17} \text{ cm}^{-3}$, (e) $1.8 \times 10^{18} \text{ cm}^{-3}$. Curves (c) and (d) are fitted by an oscillation period of 143 fs. The inset shows the spectrum of the exciting laser pulse and the energy positions of the A exciton (A), the B exciton (B), the B-continuum edge (B_c), and the B-exciton energy $+ \hbar\omega_{\text{LO}}$ ($B + \text{LO}$).

product.^{14,15} The samples are placed in a He cryostat and all data are obtained at a temperature of $T = 5$ K.

III. RESULTS AND DISCUSSION

A. Non-Markovian LO-phonon scattering

Since II-VI semiconductors possess not only a higher Fröhlich coupling but also large exciton binding energies, we expect quantum beats between the $n=1$ exciton state and exciton states with $n > 1$. Furthermore, the Coulomb correlation between excitons and continuum states should result in the well-known phenomena of local-field effects (LF) and excitation-induced dephasing (EID).^{16–25} An inherent experimental problem is therefore the superposition of all these different signals in the FWM response which is illustrated in Fig. 1. In the inset of Fig. 1 the experimental conditions can be seen which are chosen following the experiment on GaAs.⁷ The central energy of a spectrally broad laser pulse is tuned near the continuum edge and both exciton and continuum states up to $E_G + \hbar\omega_{\text{LO}}$ are excited simultaneously. Excitation of states arising from the A-exciton series has been switched off by using the polarization configuration $\vec{E} \parallel \vec{c}$ of the incident \vec{E} field. The importance of high exciton binding energies and Coulomb interaction between excitons and between exciton and continuum states is indicated by (i) the observation of quantum beats between the $B_{n=1}$ - and the $B_{n=2}$ - exciton state at lowest excitation densities [case (a) in Fig. 1; the oscillation period of 380 fs corresponds to the $1s$ - $2s$ splitting energy $\Delta E_{1s,2s} = 11$ meV], and (ii) the large signal enhancement and very fast decay at zero delay times τ , which is a clear hint to excitation-induced ultrafast coherent transients.^{23–25} With increasing excitation intensities the decay of the signal at delay times $\tau > 100$ fs becomes faster due to exciton-carrier scattering. The shift of the maximum of the FWM signal towards later times shows the transition between two different mechanisms: the change from an

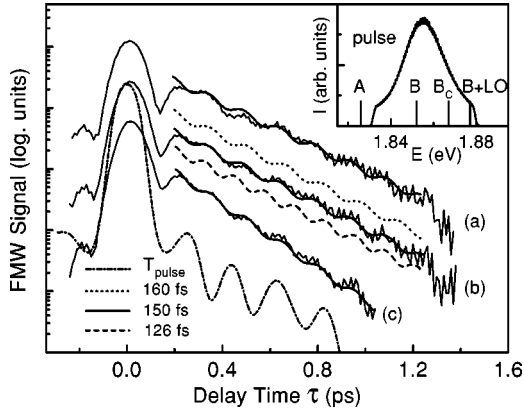


FIG. 2. Time-integrated FWM signal as a function of delay time excited by a 100 fs pulse of polarization $\vec{E} \parallel \vec{c}$ and detected at the energy of the B exciton $E_B = 1.852$ eV. The excitation densities are (a) $5 \times 10^{15} \text{ cm}^{-3}$, (b) $2 \times 10^{16} \text{ cm}^{-3}$, (c) $5 \times 10^{16} \text{ cm}^{-3}$. The inset shows the spectrum of the exciting laser pulse and the energy positions of the A exciton (A), the B exciton (B), the B -continuum edge (B_C), and the B -exciton energy $+\hbar\omega_{LO}$ ($B+LO$). The dashed-dotted line is the temporal profile of the laser pulse; the solid, dashed, and dotted lines are fits of the oscillations for different oscillation periods (see text).

excitation-induced dephasing at the exciton to a photon echolike signal arising from excitation of continuum states distributed in \vec{k} space. In the intermediate density range, i.e., under conditions where the $2s$ exciton is already screened but the $1s$ exciton signal decay is still longer than the LO-phonon period, weak oscillations of a period of 143 ± 10 fs are visible.

To enhance the signals arising from the LO-phonon quantum kinetics we use in the following an experimental configuration in which the continuum contributions are reduced. The spectral bandwidth of the exciting pulse is limited by pulse shaping between $E_B - 20$ meV and $E_B + 27$ meV around the B -exciton energy (see inset of Fig. 2). Thus we reduce the distribution of continuum states in \vec{k} space and do not allow oscillation with twice the LO-phonon period (or higher multiples) which would additionally modulate the signal. Furthermore, the formation of a density grating in the continuum is reduced.²⁵ Also, the pulse maximum is not resonant with the $B_{n=2}$ exciton (as in the setup shown in the inset of Fig. 1) which weakens the $1s$ - $2s$ beat signal. Applying this pulse shaping, the time-integrated FWM measured for different excitation densities is shown in Fig. 2. Pronounced oscillations can be seen. The fast initial decay due to EID effects is reduced and the LO-phonon oscillations can be observed over a time interval of 800 fs. To exclude any experimental artifact due to pulse shaping, the temporal shape of the excitation pulse is shown too. The oscillations in the pulse ($T_{\text{pulse}} = 192$ fs) do not coincide with the signal oscillation and are about two orders of magnitude below the oscillations of the signal.

An intuitive explanation for the oscillating FWM signal is the assumption of non-energy-conserving scattering events. If an electron at state \vec{k} is scattered to a state \vec{k}' by emission of an LO phonon but with the peculiarity that both initial and final states have the same energy (or are even identical), then a deficit in the energy balance exists of just $\hbar\omega_{LO}$. The

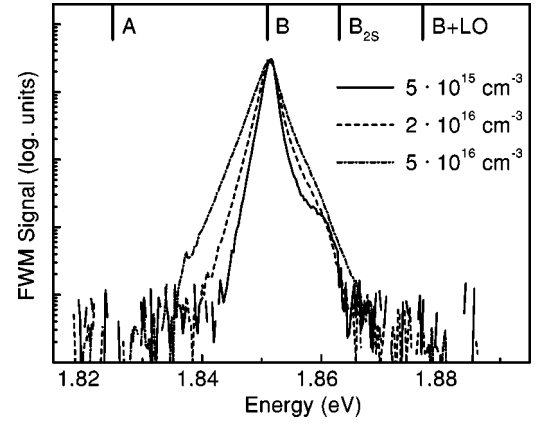


FIG. 3. Spectral response of the FWM signal shown in Fig. 2 measured at a delay time of $\tau = 0$ fs. The spectra are normalized with respect to the maximum.

temporal response of the FWM signal oscillates with that LO-phonon period until the scattering process is completed up to a maximum time which should correspond to the finite lifetime of the LO phonon. Such an oscillatory behavior of the FWM response is predicted in quantum kinetic theory.^{8,26} In contrast to Boltzmann kinetics, the information about the phases of the coherently excited polarizations is preserved after summation over all contributing interband polarizations.^{27,28} Considering only electron-LO-phonon interaction, the renormalization of T_{LO} , i.e., the difference between T_{osc} and T_{LO} has been traced back to a negligible hole-LO-phonon coupling.⁷ The different valence and conduction band dispersions result in the renormalization factor $(1 + m_e/m_h)$. Following that illustrative model, in case of exciton-LO-phonon interaction the oscillation time will change since then both electron and hole are involved in the coupling and no reason exists for any renormalization of T_{LO} . Therefore, the oscillation period provides an information about the dominant interaction pathway.

For the three different excitation densities n shown in Fig. 2, the oscillation period T_{osc} , the modulation depth a , and the decay time T_{decay} have been determined by fitting the data according to $I_{FWM} \sim [1 + a \sin(\omega_{osc}t - \phi)] \exp(-t/T_{decay})$. For the time-integrated FWM signal at $n = 5 \times 10^{15} \text{ cm}^{-3}$, $2 \times 10^{16} \text{ cm}^{-3}$, and $5 \times 10^{16} \text{ cm}^{-3}$ we find a constant modulation depth of $a = 0.13$, an oscillation period of $T_{osc} = 150 \pm 5$ fs and slightly decreasing decay times of $T_{decay} = 235$ fs, 220 fs, and 165 fs with increasing excitation density (the phase shift ϕ was the same for all curves). Both modulation depth and oscillation period are independent of intensity in the given range. For comparison, along with the measured oscillation periods and their fits, the period $T_{LO} = 160$ fs and $\bar{T}_{osc} = 126$ fs are plotted in Fig. 2. The occurrence of a fully renormalized oscillation \bar{T}_{osc} can clearly be excluded from our experiments. The deviation of T_{osc} from both $T_{LO} = 160$ fs and $\bar{T}_{osc} = 126$ fs illustrates the failure of the weak coupling theory and the demand for a different quantum kinetic treatment in case of strong coupling strengths and high excitonic binding energies. The reason for the observed deviations could be a superposition of signals arising from both exciton- and electron-LO-phonon coupling.

In Fig. 3 the spectral response of the FWM signal is plot-

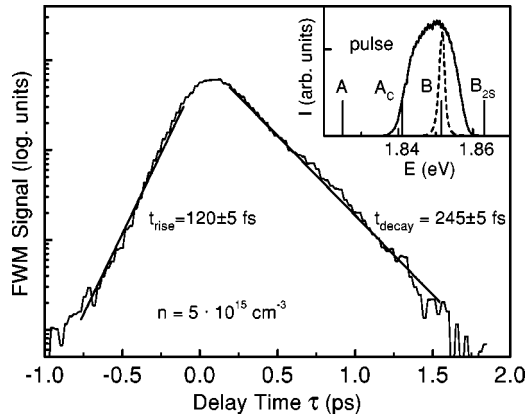


FIG. 4. Time-integrated FWM signal as a function of delay time after excitation by a pulse-shaped 210 fs pulse at $E = 1.85$ eV in the Markov limit (see text). The inset shows the spectrum of the exciting laser pulse (solid line) and the energy positions of the A exciton (A), the A -continuum edge (A_C), the B exciton (B) (dashed line, spectrum), and the energy of the $B_{n=2}$ exciton (B_{2S}).

ted for three different intensities. At lowest excitation we still have a small contribution from the $B_{n=2}$ -exciton state which vanishes with increasing density. Also the efficient suppression of the A -exciton signal by pulse shaping and $\vec{E} \parallel \vec{c}$ polarization is confirmed. With increasing intensity, the spectral response of the B exciton gradually broadens but no signal at the energy $E_B \pm \hbar \omega_{LO}$ is found, also not at different delay times τ . The same is found in the experiments shown in Fig. 1 in case of low excitation densities [curves (a)–(c)], before the continuum starts to contribute to the spectrum [curves (d) and (e) in Fig. 1]. The missing LO-phonon sidebands are not explained until now by a theory considering the strong coupling limit.

B. The Markov limit in semiconductors

The external pulse shaper can also be used to extend the exciting laser pulses up to a few hundreds of femtoseconds. In this case solely the B exciton of CdSe is excited and we can study the Markov Limit. The result is shown in Fig. 4 for resonant excitation of the B exciton by a 210 fs laser pulse and a low excitation density of $5 \times 10^{15} \text{ cm}^{-3}$. It can be summarized as follows: (i) the decay of the FWM signal shows no oscillations and is almost monoexponential with a decay time of $T_{\text{decay}} = 246$ fs (which would result in a homogeneous linewidth $\Gamma = 2.7$ meV in case of a Lorentzian line shape), (ii) the linewidth of the spectral response is 1.8 meV (FWHM, see inset of Fig. 4), i.e., the relation $\Gamma = 2\hbar/T_2$ is not fulfilled, and (iii) signals at negative delay times are observed. These features illustrate the well-known fact that even for spectrally narrow, resonant excitation of a single exciton, the Markov limit in semiconductors does not result in a system which can be described by a two-band optical Bloch equation without accounting for Coulomb interaction. The observation of strong FWM signals at negative delay times indicate the dominance of interaction-induced signals (LF and EID) caused by Coulomb correlation effects in the semiconductor sample. For a homogeneously broadened resonance the relation $t_{\text{rise}} = t_{\text{decay}}/2$ is expected,¹⁶ in agreement with our observations at low excitation densities (n

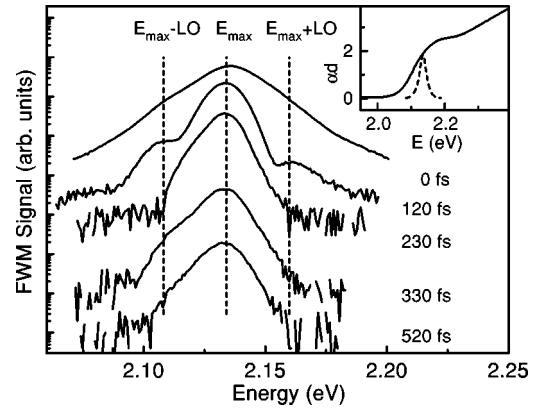


FIG. 5. Spectral FWM response of a $R = 2.5$ nm CdSe quantum dot sample measured at different delay times, as indicated, for excitation with 80 fs pulses centered at $E = 2.134$ eV. The inset shows the linear absorption spectrum of the CdSe quantum dots embedded in glass and the laser pulse (dashed).

$= 2 \times 10^{15} \text{ cm}^{-3}$ up to $n = 1.7 \times 10^{16} \text{ cm}^{-3}$). The difference between decay time and spectral FWM linewidth is due to the different real-time dynamics of the signals arising from excitation-induced dephasing and phase-space filling. The EID signal results in a Lorentz-squared line shape having a linewidth of 64% of the Lorentzian linewidth in agreement with our results. The fast decay time is attributed to the coupling of the B -exciton to A -continuum states.

C. Comparison between bulk CdSe and CdSe quantum dots

Quantum dots are of nanometer size and have only a few discrete energy states. The lack of continuum states and the tiny, limited volume of spherical or slightly prolate shape make them different from bulk semiconductors. In quantum dots, no real energy states exist which are resonant to $E \pm \hbar \omega_{LO}$ with E the quantum confined energy level. A coupling to coherent LO phonons is assumed for quantum dots. In this case, the crystal lattice itself is driven by an external laser field to coherent oscillations which couple then to an electronic state and modulate its polarization decay. The excitation of one electron-hole pair per dot could be already sufficient to achieve a high local charge density within a nanometer-sized crystal lattice. Such a process, however, should strongly depend on excitation density because it needs high local charge densities to produce the strong lattice distortions. This intensity dependence can be used to divide between LO-phonon quantum kinetics and coupling to coherent lattice oscillation with T_{LO} , as outlined in a recent paper and demonstrated in coherent control experiments.¹¹ Carrying out a three-beam FWM experiment, oscillations of a period of 163 fs have been reported in Refs. 29 and 30 for CdSe quantum dots. However, a simultaneous analysis of the temporal and spectral response of the FWM signal has not been performed yet. In case of coupling to coherent LO phonons, oscillations with exactly the LO phonon period and sidebands in the optical spectra are expected which exhibits a constant spectral shape over time. The modulation depth of the oscillations should increase with increasing intensity. As shown this was not observed in the case of LO-phonon quantum kinetics in bulk CdSe.

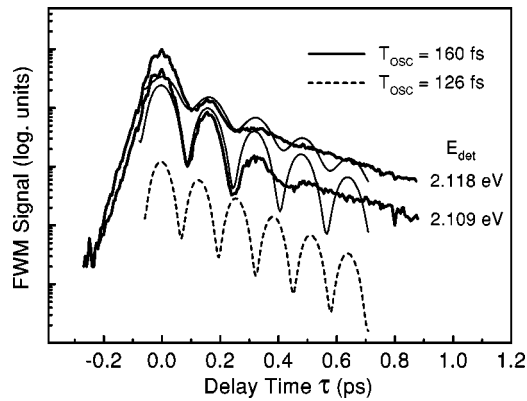


FIG. 6. Time-integrated FWM signal as a function of delay time excited by 80 fs pulses and detected at two different energies $E = 2.118$ eV and $E = 2.109$ eV. The solid lines are fits reproducing the oscillation frequency of $T_{LO} = 160$ fs and the dashed line illustrates an oscillation with $\bar{T}_{LO} = 126$ fs.

In this section we investigate both the temporal and spectral FWM response of CdSe quantum dots embedded in a glass matrix and compare the results with those of bulk CdSe obtained under similar experimental conditions. The inset in Fig. 5 shows the linear absorption spectrum for the $R = 2.5$ nm quantum dot sample under study. For such a size, the confined electron-hole pair ground state and first excited state are separated in energy by ~ 70 meV.³¹ The spectral response of the two-beam four-wave mixing experiment is shown in Fig. 5 for different delay times τ . In contrast to bulk CdSe, two sidebands are visible separated from the signal maximum by approximately the LO-phonon energy. The corresponding delay-time traces of the time-integrated FWM signal are shown in Fig. 6 for two different spectral positions. In particular at the low-energy side (within the tail of size distribution) we see pronounced oscillations which can be fitted well by a period $T_{osc} = 160 \pm 3$ fs, in agreement with the result of Ref. 30. The damping of the oscillations, however, is stronger as observed for colloidal CdSe nanocrystals, most probably caused by the inclusion of the quantum dots in a glass matrix. The phonon oscillations here are damped by a rate of $\sim (1/300)$ fs⁻¹, which is also about twice the

value measured for bulk CdSe. Added to the plot is the corresponding curve for the renormalized oscillation period $\bar{T}_{osc} = 126$ fs which clearly does not agree with the experimental data for CdSe quantum dots. When the excitation density is varied over 1.5 orders of magnitude, *no* change in the oscillation time and modulation depth is observed.

It should be noted that an inhomogeneous broadening can result in signal modulations both in the spectral and temporal response. This effect has been examined and found not to explain our experimental results because it does not result in temporal oscillations of the FWM signal.

IV. SUMMARY

The experiments show the features of quantum kinetics in highly polar, wide-gap semiconductors. The oscillation period T_{osc} between \bar{T}_{osc} and T_{LO} and the spectral response cannot be explained by present theories and indicate the importance of the excitonic binding for quantum kinetics. The experiments under conditions of the Markov limit illustrate the typical features of optical nonlinearities in semiconductors, i.e., local-field effects and excitation-induced dephasing. By comparing the results of the temporal and spectral response obtained for bulk CdSe and CdSe quantum dots we found for quantum dots an oscillation period with exactly the LO-phonon oscillation time and sidebands in the spectra, whereas for bulk material a slightly smaller oscillation period and no sidebands are observed within a detection range of four orders of magnitude. However, in both materials the modulation depth in the oscillating FWM signal is within 1.5 orders of magnitude, independent of excitation intensity. The latter result implies that both in CdSe quantum dots and bulk CdSe, interaction with light does not result in a strong non-equilibrium population of coherent phonons.

ACKNOWLEDGMENTS

Stimulating discussions with M. Wegener, H. Haug and L. Banyai are grateful acknowledged. Financial support of the Deutsche Forschungsgemeinschaft within the program “Quantum Coherence in Semiconductors” and by the Ministry of Education and Science of Nordrhein-Westfalia is grateful acknowledged.

- ¹ L. Allen and J.H. Eberly, *Optical Resonances and Two-Level Atoms* (Wiley, New York, 1975).
- ² Y.R. Shen, *The Principles of Nonlinear Optics* (Wiley, New York, 1984).
- ³ P. Meystre and M. Sargent III, *Elements of Quantum Optics* (Springer, Berlin, 1991).
- ⁴ H. Haug and J.-P. Jauho, *Quantum Kinetics in Transport and Optics of Semiconductors*, Springer Series in Solid State Sciences No. 123 (Springer-Verlag, Berlin, 1996).
- ⁵ E.T.J. Nibbering, A. Wiersma, and K. Duppen, *Phys. Rev. Lett.* **66**, 2464 (1991).
- ⁶ B. Fainberg, *Phys. Rev. A* **48**, 849 (1993).
- ⁷ L. Banyai, D.B. Tran Thoai, E. Reitsamer, H. Haug, D. Steinbach, M.U. Wehner, M. Wegener, T. Marschner, and W. Stolz, *Phys. Rev. Lett.* **75**, 2188 (1995).

- ⁸ D.T. Thoai and H. Haug, *Phys. Rev. B* **47**, 3574 (1993); L. Banyai, E. Reitsamer, D.B. Tran Thoai, and H. Haug, *J. Opt. Soc. Am. B* **13**, 1278 (1996).
- ⁹ C. Fürst, A. Leitenstorfer, A. Laubereau, and R. Zimmermann, *Phys. Rev. Lett.* **78**, 3733 (1997).
- ¹⁰ M. Wegener, M.U. Wehner, D. Steinbach, M.H. Ulm, G. Kocherscheidt, and D.S. Chemla, *Adv. Solid State Phys.* **38**, 297 (1999).
- ¹¹ M.U. Wehner, M.H. Ulm, D.S. Chemla, and M. Wegener, *Phys. Rev. Lett.* **80**, 1992 (1998); M.U. Wehner, D.S. Chemla, and M. Wegener, *Phys. Rev. B* **58**, 3590 (1998).
- ¹² C. Dörnfeld and J. M. Hvam, *IEEE J. Quantum Electron.* **25**, 904 (1989).
- ¹³ J. M. Hvam, C. Dörnfeld, and H. Schwab, *Phys. Status Solidi B* **150**, 387 (1988).

- ¹⁴ C. Froehly, B. Colombeau, and M. Vampouille, in *Progress in Optics*, edited by E. Wolf (North-Holland, Amsterdam, 1983), Vol. XX, pp. 65–153.
- ¹⁵ A.M. Weiner, J.P. Heritage, and E.M. Kirschner, *J. Opt. Soc. Am. B* **5**, 1563 (1988).
- ¹⁶ M. Wegener, D.S. Chemla, S. Schmitt-Rink, and W. Schäfer, *Phys. Rev. A* **42**, 5675 (1990).
- ¹⁷ K. Leo, M. Wegener, J. Shah, D.S. Chemla, E. Göbel, T. Damen, S. Schmitt-Rink, and W. Schäfer, *Phys. Rev. Lett.* **65**, 1340 (1990).
- ¹⁸ D. Kim, J. Shah, T. Damen, W. Schäfer, F. Jahnke, S. Schmitt-Rink, and K. Köhler, *Phys. Rev. Lett.* **69**, 2725 (1992).
- ¹⁹ S. Weiss, M. Mycek, J. Bigot, S. Schmitt-Rink, D.S. Chemla, *Phys. Rev. Lett.* **69**, 2685 (1992).
- ²⁰ J. Feldmann, T. Meier, G.v. Plessen, M. Koch, E. Göbel, P. Thomas, G. Bacher, C. Hartmann, H. Schweizer, W. Schäfer, and H. Nickel, *Phys. Rev. Lett.* **70**, 3027 (1993).
- ²¹ T. Rappen, U.G. Peter, M. Wegener, and W. Schäfer, *Phys. Rev. B* **49**, 10 774 (1994).
- ²² H. Wang, K. Ferrio, D. Steel, P. Berman, Y. Z. Hu, R. Binder, and S.W. Koch, *Phys. Rev. A* **49**, R1551 (1994).
- ²³ D. Birkedal, V.G. Lyssenko, J.M. Hvam, and K. El Sayed, *Phys. Rev. B* **54**, R14 250 (1996).
- ²⁴ M.U. Wehner, D. Steinbach, and M. Wegener, *Phys. Rev. B* **54**, R5211 (1996).
- ²⁵ K. El Sayed, D. Birkedal, V.G. Lyssenko, and J.M. Hvam, *Phys. Rev. B* **55**, 2456 (1997).
- ²⁶ D.B. Tran Thoai and H. Haug, *Phys. Status Solidi B* **188**, 387 (1995).
- ²⁷ T. Kuhn and F. Rossi, *Phys. Rev. Lett.* **69**, 977 (1992).
- ²⁸ J. Schilp, T. Kuhn, and G. Mahler, *Phys. Rev. B* **50**, 5435 (1994).
- ²⁹ R.W. Schoenlein, D.M. Mittleman, J.J. Shiang, A.P. Alivisatos, and C.V. Shank, *Phys. Rev. Lett.* **70**, 1014 (1993).
- ³⁰ D.M. Mittleman, R.W. Schoenlein, J.J. Shiang, V.L. Colvin, A.P. Alivisatos, and C.V. Shank, *Phys. Rev. B* **49**, 14 435 (1994).
- ³¹ U. Woggon, O. Wind, F. Gindele, E. Tsitsishvili, and M. Müller, *J. Lumin.* **70**, 269 (1996).